

CMF: CASCADED MULTI-MODEL FUSION FOR REFERRING IMAGE SEGMENTATION

Jianhua Yang¹, Yan Huang², Zhanyu Ma^{1,3}, Liang Wang^{2,4,5}

¹ PRIS Lab., School of Artificial Intelligence, Beijing University of Posts and Telecommunications

²Center for Research on Intelligent Perception and Computing (CRIPC), National Laboratory of Pattern Recognition (NLPR), Institute of Automation, Chinese Academy of Sciences (CASIA)

³Beijing Academy of Artificial Intelligence, Beijing, China

⁴Artificial Intelligence Research, Chinese Academy of Sciences (AIR-CAS)

⁵School of Artificial Intelligence, University of Chinese Academy of Sciences

ABSTRACT

In this work, we address the task of referring image segmentation (RIS), which aims at predicting a segmentation mask for the object described by a natural language expression. Most existing methods focus on establishing unidirectional or directional relationships between visual and linguistic features to associate two modalities together, while the multi-scale context is ignored or insufficiently modeled. Multi-scale context is crucial to localize and segment those objects that have large scale variations during the multi-modal fusion process. To solve this problem, we propose a simple yet effective Cascaded Multi-modal Fusion (CMF) module, which stacks multiple atrous convolutional layers in parallel and further introduces a cascaded branch to fuse visual and linguistic features. The cascaded branch can progressively integrate multi-scale contextual information and facilitate the alignment of two modalities during the multi-modal fusion process. Experimental results on four benchmark datasets demonstrate that our method outperforms most state-of-the-art methods. Code is available at <https://github.com/jianhua2022/CMF-Refseg>.

Index Terms— Referring Image Segmentation, Natural Language Expression, Context Modeling

1. INTRODUCTION

Referring image segmentation (RIS) [1] is a challenging task which associates semantics of natural language expressions with contents of images. As illustrated in Fig.1, given an image and a natural language expression, the goal of RIS is to predict a binary mask for the object specified by the expression. The categories of semantic segmentation are predefined and fixed, while RIS can take arbitrary expressions as input to

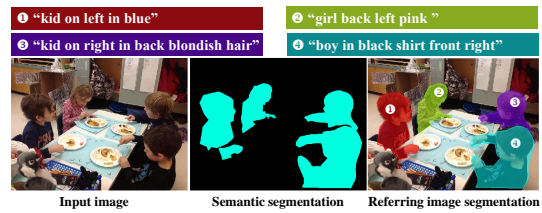


Fig. 1: Illustration of referring image segmentation, which aims at segmenting the object specified by a natural language expression.

describe the object of interest. The expressions may contain diverse semantic concepts, such as entities, attributes and actions. Thus, how to align these semantic concepts with visual contents is a main challenge of this task.

Previous works [1, 2, 3] usually concatenated visual and linguistic features extracted from the convolutional neural network (CNN) and long short-term memory (LSTM) [4] network respectively, and then predicted the mask from integrated multi-modal features via a fully convolutional network (FCN) [5]. These works ignored the linguistic variations of input expressions, and treated each word equally to each visual region. Thus it is hard to accurately distinguish the referred object from the background. Some works applied dynamic filters [6] or word attention [7] to learn adaptive expression representations but lacked interactions between vision and language. Interactions between two modalities can associate each word with each image region, and further highlight the features of the target object for accurate segmentation. Recent works proposed to model the interactions by introducing unidirectional [8, 9] or bi-directional [10] attention mechanisms.

Although promising results have been achieved in these works, the multi-scale visual context in the multi-modal fusion process has not been explored. Multi-scale context modeling has verified its effectiveness on boosting the segmentation accuracy of objects in semantic segmentation [11, 12, 13, 14]. Recent works also have shown that the performance of RIS can be further improved through aggregating long-range context from concatenated visual and linguistic features [15]

This work was jointly supported by National Key Research and Development Program of China Grant No. 2018AAA0100400, National Natural Science Foundation of China (61525306, 61633021, 61721004, 61806194, U1803261, 61976132, 61922015, 61773071, and U19B2036), Beijing Nova Program (Z201100006820079), Shandong Provincial Key Research and Development Program (2019JZZY010119), Key Research Program of Frontier Sciences CAS Grant No. ZDBS-LY-JSC032, CAS-AIR, and in part by Beijing Natural Science Foundation Project under Grant Z200002.

with self-attention [16], or collecting multi-scale context from fused multi-model features [10, 17] with atrous spatial pyramid pooling (ASPP) [11, 18]. However, the former is high memory cost for computing the affinity map and may introduce redundant features, which are harmful to distinguish the referred object. The latter captures multi-scale context after two modalities are fused. The fused multi-modal features may contain heterogeneous noises from two modalities, which result in the model cannot adaptively learn the scale variations of objects. Different from these works, we argue that the multi-scale contextual information is important to facilitate the alignment of two modalities and correctly localize the referred object during the multi-modal fusion process.

In this paper, we focus on multi-scale context modeling during vision and language fusion process rather than after fused multi-modal features. Specifically, we propose a Cascaded Multi-modal Fusion (CMF) module, which can effectively aggregate multi-scale contextual information into multi-modal fusion process and encourage two modalities alignment at each position of fused feature map. The module is based on ASPP and further introduces a cascaded multi-modal fusion branch, where we iteratively fuse visual and linguistic features with atrous convolutional layers with gradually increased dilated rates. Besides, to integrate the fused multi-modal features from different layers of visual backbone for segmentation mask refining, we introduce a bi-directionally convolutional gated recurrent unit (GRU) [19] to fuse them from top-down and bottom-up paths. Finally, we conduct extensive experiments on four benchmark datasets to validate our proposed method. Experimental results show that our method outperforms most state-of-the-art methods.

2. RELATED WORK

Referring Image Segmentation (RIS). RIS aims at segmenting the object specified by a natural language expression. Hu *et al.* [1] made the first effort for this task via a direct concatenation of visual and linguistic features from CNN and LSTM. In order to associate visual regions with individual words and highlight features of the target object, unidirectional and bi-directional interactions between visual and linguistic features have been explored by attention mechanism [8, 7, 15, 10, 9, 17]. Multi-level feature aggregation [3, 15, 10], generative adversarial learning [20], and query reconstruction [21] were also investigated to refine multi-modal features and further improve the performance of segmentation. However, these works ignore or ineffectively model multi-scale context during multi-modal fusion process, where the context is crucial to align two modalities and accurately segment the objects with large scale variations. Different from them, our work focuses on multi-scale context modeling in an effective way during the multi-modal fusion process.

Context Modeling. Modeling the multi-scale contextual information plays a key role in semantic segmentation. PSP-

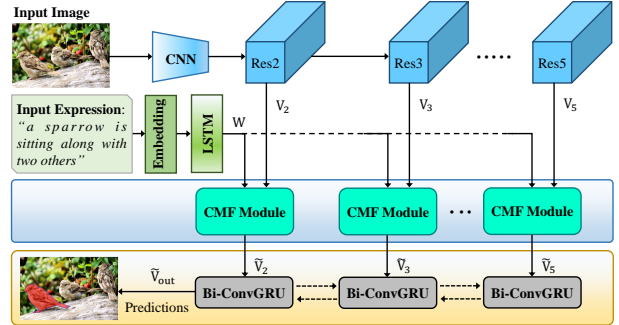


Fig. 2: Illustration of the overall architecture. It consists of three parts: vision and language encoders, Cascaded Multi-modal Fusion (CMF) module and a Bi-ConvGRU.

Net [13] collected context from different scales via a spatial pyramid pooling (SPP) module. ASPP [11, 18] stacked multiple parallel atrous convolutional layers with different dilated rates to capture multi-scale context. DANet [14] utilized a position attention and a channel attention with self-attention mechanism to aggregate long-range context. These approaches are proposed to solve the semantic segmentation rather than RIS task. Our work aims at modeling multi-scale context to improve the segmentation accuracy of referred objects in RIS task, which is more challenging than semantic segmentation.

3. THE PROPOSED METHOD

The overall architecture of our proposed model is illustrated in Fig. 2. The visual and linguistic features are firstly extracted using a CNN and a one-layer LSTM respectively, and then fed into Cascaded Multi-modal Fusion (CMF) module to fuse them. Finally, a Bi-ConvGRU is introduced to refine the fused multi-modal features from different layers of CNN. The details will be elaborated in the following.

3.1. Visual and Linguistic Feature Extraction

Our model takes an image and a referring expression as inputs. The visual features V_l ($l=2,3,4,5$) are extracted from the corresponding layers of *Res2*, *Res3*, *Res4* and *Res5* in the CNN backbone. Then we transform these features into the same size, *i.e.*, $V_l \in \mathbb{R}^{h \times w \times D_v}$. For an expression with T words, we embed each word with the Glove [22], and then employ a one-layer LSTM to encode the word embedding sequence. Finally, all words in an expression are represented with their corresponding LSTM hidden states and denoted as $L \in \mathbb{R}^{T \times D_w}$. Following prior works [1, 2], we also introduce an 8-D spatial coordinate feature $S \in \mathbb{R}^{h \times w \times 8}$ to enhance the position reasoning of the model.

3.2. Cascaded Multi-modal Fusion (CMF) Module

As prior works [1, 2, 3], the heterogeneous features from two modalities are concatenated and followed by a 1×1 convolutional layer to fuse them. However, such a simple multi-modal fusion manner ignored the linguistic variations of input expressions and treated each pixel individually without considering the multi-scale contextual information during the

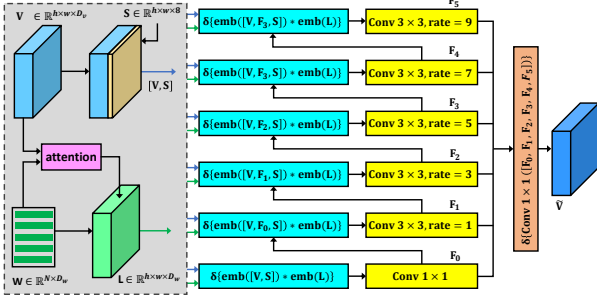


Fig. 3: The cascaded multi-modal fusion (CMF) module. $emb(\cdot)$ denotes 1×1 convolutional layer, $\delta(\cdot)$ is ReLU function, $*$ means Hadamard product.

multi-modal fusion process. Thus, we propose a CMF module to fuse two modalities by taking linguistic variations and multi-scale contextual information into account.

The details of the CMF module is shown in Fig.3. Concretely, to learn more robust linguistic representation and eliminate the effect of linguistic variations, we first introduce an image-to-word attention to compute the relevance between each word and each visual region, then utilize the calculated attention matrix followed by a softmax layer to compute the weighted summation of originally linguistic features. For the i -th visual region and the t -th word, the attention matrix is calculated by:

$$A_{i,t} = \text{softmax}[(W_v v_i)^T (W_h h_t)], \quad (1)$$

then the updated linguistic representation L for the visual feature map V is $L = \{l_i\} \in \mathbb{R}^{h \times w \times D_w}$, where l_i is calculated by:

$$l_i = \sum_{t=1}^T A_{i,t} h_t. \quad (2)$$

To capture multi-scale contextual information, the original ASPP [11, 18] stacks multiple parallel 3×3 convolutional layers with different dilated rates and further fuses them with concatenation followed by an 1×1 convolutional layer. To effectively model multi-scale context and facilitate alignment of two modalities for RIS task, we introduce a cascaded fusion branch on original ASPP, as shown in Fig.3. This branch first fuses two modalities with an 1×1 convolutional layer, and then iteratively fuses two modalities using atrous convolutional layers with gradually increased dilated rates. More specifically, for the n -th fusion layer in the cascaded branch, we first concatenate the input visual feature V , spatial feature S and the fusion result F_{n-1} from the $(n-1)$ -th fusion layer, which can be denoted as $[V, S, F_{n-1}]$. Then we apply two linearly embedding layers (*i.e.*, 1×1 convolutional layers) to transform the concatenated features and updated linguistic representation into the same dimension. Instead of concatenation similar to previous works [1, 2, 3], here we combine two types of features with Hadamard product followed by a non-linear projection. Finally, we feed the combined multi-modal features into a 3×3 convolutional layers with a specific dilated rate to fuse them. By introducing such a cascaded fusion module, the visual contextual information is gradually integrated into multi-modal fusion process in cascaded and parallel directions of CMF module.

3.3. Multi-level Feature Fusion and Mask Prediction

Previous approaches [3, 15, 9, 10] have shown that integrating multi-modal features from different levels of CNN can further improve the accuracy of segmentation masks. In our work, we introduce a bi-directionally convolutional GRU (Bi-ConvGRU) to progressively integrate the fused multi-modal features in bottom-up and top-down manners, which is corresponding to the two directions of forward and backward paths. The top-down manner can enhance the lower-level features with rich semantics, while the bottom-up manner can compensate spatial details for higher-level features with lower-level ones. The output of the Bi-ConvGRU is formulated as:

$$\tilde{V}_{out} = \text{ReLU}(W_p^{\vec{H}} \vec{H}_l + W_p^{\overleftarrow{H}} \overleftarrow{H}_l + b), \quad (3)$$

where \vec{H} and \overleftarrow{H} denote the last hidden states of two directions, b is the bias term, and $\tilde{V}_{out} \in \mathbb{R}^{h \times w \times D_o}$ is the integrated multi-modal features. Finally, the same decoder layers and binary cross-entropy loss as previous works [3, 10] are adopted to predict the segmentation mask and optimize the network, respectively.

4. EXPERIMENTS

4.1. Experiment Settings

Datasets and Protocols. We perform experiments on four benchmark datasets, including ReferIt [23], G-Ref [24], UNC [25] and UNC+ [25]. The ReferIt contains 130,525 expressions for 96,654 regions in 19,894 images, the categories of regions are objects or stuff (*e.g.*, “sky”, “wall”). The G-Ref consists of 26,711 images with 104,560 expressions for 54,822 objects. The average length of expressions (8.4 words) in this dataset is much longer than that of other three datasets. The UNC contains 142,209 expressions for 50,000 objects in 19,994 images. The UNC+ is composed of 141,564 expressions for 49,856 objects in 19,992 images and focuses on appearance-based descriptions. Similar to [1, 2], the overall Intersection-over-Union (IoU), which calculates total intersection region over total union regions of all test images, is adopted to evaluate our model. We also report the precision at difference threshold, *i.e.*, $P@X$ ($X \in \{0.5, 0.6, 0.7, 0.8, 0.9\}$).

Implementation Details. Similar to [2, 3], the commonly used DeepLab ResNet-101 [11], which is pre-trained on Pascal VOC [26], is utilized as our CNN backbone to extract different level visual features. This backbone is fixed during training and testing. The input images are resized to 320×320 . For language encoding, we first keep the maximum length of each expression as 20. The network is trained using Adam optimizer with an initial learning rate of $2.5e^{-4}$ and a weight decay of $5e^{-4}$. We apply a polynomial decay with power of 0.9 to the learning rate. For the feature dimensions, we set $D_v = D_w = 1000$, $D_o = 500$.

4.2. Comparison with the State-of-the-arts

We conduct experiments on four benchmark datasets and compare the corresponding results with previous methods in Table 1. Note that the symbol “ \star ” denotes the segmentation

Table 1: Comparisons with the state-of-the-art methods on four datasets. “*” denotes the results are post-processed with DenseCRF.

Methods	UNC			UNC+			G-Ref	ReferIt
	val	testA	testB	val	testA	testB	val	test
LSTM-CNN (2016) [1]	-	-	-	-	-	-	28.14	48.03
RMI* (2017) [2]	45.18	45.69	45.57	29.86	30.48	29.50	34.52	58.73
RRN* (2018) [3]	55.33	57.26	53.95	39.75	42.15	36.11	36.45	63.63
ASGN (2019) [20]	50.46	51.20	49.27	38.41	39.79	35.97	41.36	60.31
CMSA* (2019) [15]	58.32	60.61	55.09	43.76	47.60	37.89	39.98	63.80
DCLSTM* (2020) [7]	59.04	60.74	56.73	44.54	47.92	39.73	41.77	63.92
CGAN (2020) [17]	59.25	62.37	53.94	46.16	51.37	38.24	46.54	-
QRN (2020) [21]	59.75	60.96	58.77	48.23	52.65	40.89	42.11	65.22
STEP (2019) [9]	60.04	63.46	57.97	48.19	52.33	40.41	46.40	64.13
BRINet* (2020) [10]	61.35	63.37	59.57	48.57	52.87	42.13	48.04	63.46
Ours	61.69	64.33	59.76	49.38	53.47	42.05	45.40	64.67
Ours*	62.03	64.70	60.10	49.62	53.85	42.22	45.65	64.72

results of the corresponding method are post-processed with DenseCRF [27]. It can be observed that the performance of our method outperforms all previous methods on UNC and UNC+. Compared with the best method BRINet, our method achieves 0.68%, 1.33% and 0.5% improvement on val, testA and testB sets of UNC, 1.05%, 0.98% and 0.09% improvement on val, testA and testB sets of UNC+. In particular, the expression of UNC+ does not include location words, the experimental results show that our method is robust to align the semantics of objects between two modalities. Since G-Ref tends to describe an object with a long expression, and ReferIt contains stuff categories, they are more challenging than UNC and UNC+. Although our method does not establish complex interactions between two modalities like [9, 17, 10], the performance of our method also outperforms most state-of-the-art methods on G-Ref and ReferIt. Thus, the integration of multi-scale context information is helpful to align two modalities and improve segmentation accuracy of objects.

4.3. Ablation Study

Table 2: Ablation study on the UNC val set with the visual feature V_5 (post-processed by DenseCRF).

Method	P@0.5	P@0.6	P@0.7	P@0.8	P@0.9	IoU
RRN [3]	46.82	36.47	25.25	12.25	1.67	46.87
CMSA [15]	51.95	43.11	32.74	19.28	4.11	50.12
DCLSTM [7]	54.62	44.20	30.77	16.02	2.56	50.50
BRINet [10]	65.53	57.46	46.85	30.42	7.28	56.76
Baseline	48.15	38.56	28.11	16.58	3.81	48.13
Baseline + ATTN	50.54	41.20	30.13	17.74	4.36	49.50
Baseline + ATTN + ASPP	61.48	53.61	43.47	28.49	7.41	55.30
CMF Module	68.60	62.35	52.35	36.40	10.23	59.05

Table 3: The impact of stacking 3×3 convolutional layers with different dilated rates in CMF module (post-processed by DenseCRF).

Methods	P@0.5	P@0.6	P@0.7	P@0.8	P@0.9	IoU
Ours (Conv 1×1)	50.54	41.20	30.13	17.74	4.36	49.50
Ours (R = 1)	53.45	44.63	34.00	21.14	5.37	51.09
Ours (R = 1,3)	59.61	51.46	41.21	26.93	7.20	54.21
Ours (R = 1,3,5)	64.02	56.42	46.40	31.67	8.76	56.72
Ours (R = 1,3,5,7)	67.66	60.71	51.29	35.32	9.97	58.48
Ours (R = 1,3,5,7,9)	68.60	62.35	52.35	36.40	10.23	59.05
Ours (R = 1,3,5,7,9,11)	69.33	62.91	53.04	37.50	10.97	59.26
Ours (R = 1,3,5,7,9,11,13)	70.00	63.25	53.38	37.07	10.64	59.41

Table 4: The impact of integrating fused multi-modal features from different levels with Bi-ConvGRU (post-processed by DenseCRF).

Methods	P@0.5	P@0.6	P@0.7	P@0.8	P@0.9	IoU
$m=\{\tilde{V}_5\}$	68.60	62.35	52.35	36.40	10.23	59.05
Bi-GRU, $m=\{\tilde{V}_5, \tilde{V}_4\}$	72.06	65.04	54.74	37.04	10.17	61.04
Bi-GRU, $m=\{\tilde{V}_5, \tilde{V}_4, \tilde{V}_3\}$	71.78	65.53	56.25	40.75	13.20	61.50
Bi-GRU, $m=\{\tilde{V}_5, \tilde{V}_4, \tilde{V}_3, \tilde{V}_2\}$	72.55	66.07	56.90	41.42	13.24	62.03

In order to verify the effectiveness of our CMF module, we first conduct ablation studies without Bi-ConvGRU on UNC val set. As [1, 2, 3], we take V_5 from *Res5* as the visual feature and fuse it with the linguistic feature. Here we consider three variants of CMF module: (1) Baseline: Following [1, 3], this model uses the last hidden state of LSTM as the holistic representation of an expression. We use Hadamard product followed by a convolutional layer with filter size 1 to fuse two modalities. (2) Baseline + Attention (ATTN): This model uses visual feature as a guidance to adaptively learn a robust linguistic representation with an attention mechanism. (3) Baseline + ATTN + ASPP: This model introduces an original ASPP model on the fused multi-modal feature, similar to [17, 10]. The experimental results are summarized in Lines 5-8 of Table 2. It can be observed that CMF module brings 10.92% improvement on baseline model, and brings 3.75% improvement compared with directly using original ASPP. Besides, we also compare CMF module with previous methods only using visual features of V_5 , which are shown in Line 1-4 of Table 2. We observe that CMF module outperforms the second best by 2.29% when only use the visual feature of V_5 .

We further study the impact of 3×3 convolutional layers with gradually increased dilated rate R in the cascaded branch, the results are shown in Table 3. We observe that by stacking convolutional layers with bigger dilated rates, the IoU is increased clearly. When we stack five convolutional layers with corresponding dilated rates as $R = \{1, 3, 5, 6, 9\}$, the IoU is improved by 10.08% compared with the model only uses an 1×1 convolutional layer. The improvement slows down by stacking more convolutional layers of bigger dilated rates, thus in our model we stack five convolutional layers with dilated rates as $R = \{1, 3, 5, 7, 9\}$. Finally, we conduct experiments to verify the relative contributions of the introduced Bi-ConvGRU for the fusion of multi-modal feature from different levels. As presented in Table 4, when we gradually integrate more fused multi-modal features from lower levels, the segmentation performance is increased.

5. CONCLUSIONS

We have proposed an effective cascaded multi-modal fusion (CMF) module for referring image segmentation. It stacks multiple atrous convolutional layers in parallel and further introduces a cascaded branch to fuse visual and linguistic features using these layers with gradually increased dilated rates. The model can iteratively integrate multi-scale context and facilitate the alignment of two modalities during multi-modal fusion process. We perform experiments on four benchmark datasets and achieve state-of-the-art performance.

6. REFERENCES

- [1] Ronghang Hu, Marcus Rohrbach, and Trevor Darrell. Segmentation from natural language expressions. In *ECCV*, pages 108–124. Springer, 2016.
- [2] Chenxi Liu, Zhe Lin, Xiaohui Shen, Jimei Yang, Xin Lu, and Alan Yuille. Recurrent multimodal interaction for referring image segmentation. In *ICCV*, pages 1271–1280, 2017.
- [3] Ruiyu Li, Kaican Li, Yi-Chun Kuo, Michelle Shu, Xiaojuan Qi, Xiaoyong Shen, and Jiaya Jia. Referring image segmentation via recurrent refinement networks. In *CVPR*, pages 5745–5753, 2018.
- [4] Sepp Hochreiter and Jürgen Schmidhuber. Long short-term memory. *Neural computation*, 9(8):1735–1780, 1997.
- [5] Jonathan Long, Evan Shelhamer, and Trevor Darrell. Fully convolutional networks for semantic segmentation. In *CVPR*, pages 3431–3440, 2015.
- [6] Edgar Margffoy-Tuay, Juan C Pérez, Emilio Botero, and Pablo Arbeláez. Dynamic multimodal instance segmentation guided by natural language queries. In *ECCV*, pages 630–645, 2018.
- [7] Linwei Ye, Zhi Liu, and Yang Wang. Dual convolutional lstm network for referring image segmentation. *TMM*, 22(12):3224–3235, 2020.
- [8] Hengcan Shi, Hongliang Li, Fanman Meng, and Qingbo Wu. Key-word-aware network for referring expression image segmentation. In *ECCV*, pages 38–54, 2018.
- [9] Ding-Jie Chen, Songhao Jia, Yi-Chen Lo, Hwann-Tzong Chen, and Tyng-Luh Liu. See-through-text grouping for referring image segmentation. In *ICCV*, pages 7454–7463, 2019.
- [10] Zhiwei Hu, Guang Feng, Jiayu Sun, Lihe Zhang, and Huchuan Lu. Bi-directional relationship inferring network for referring image segmentation. In *CVPR*, pages 4424–4433, 2020.
- [11] Liang-Chieh Chen, George Papandreou, Iasonas Kokkinos, Kevin Murphy, and Alan L Yuille. Deeplab: Semantic image segmentation with deep convolutional nets, atrous convolution, and fully connected crfs. *TPMAI*, 40(4):834–848, 2017.
- [12] Wei Liu, Andrew Rabinovich, and Alexander C Berg. Parsenet: Looking wider to see better. *arXiv preprint arXiv:1506.04579*, 2015.
- [13] Hengshuang Zhao, Jianping Shi, Xiaojuan Qi, Xiaogang Wang, and Jiaya Jia. Pyramid scene parsing network. In *CVPR*, pages 2881–2890, 2017.
- [14] Jun Fu, Jing Liu, Haijie Tian, Yong Li, Yongjun Bao, Zhiwei Fang, and Hanqing Lu. Dual attention network for scene segmentation. In *CVPR*, pages 3146–3154, 2019.
- [15] Linwei Ye, Mrigank Rochan, Zhi Liu, and Yang Wang. Cross-modal self-attention network for referring image segmentation. In *CVPR*, pages 10502–10511, 2019.
- [16] Ashish Vaswani, Noam Shazeer, Niki Parmar, Jakob Uszkoreit, Llion Jones, Aidan N Gomez, Lukasz Kaiser, and Illia Polosukhin. Attention is all you need. In *NeurIPS*, pages 5998–6008, 2017.
- [17] Gen Luo, Yiyi Zhou, Rongrong Ji, Xiaoshuai Sun, Jinsong Su, Chia-Wen Lin, and Qi Tian. Cascade grouped attention network for referring expression segmentation. In *ACM MM*, pages 1274–1282, 2020.
- [18] Liang-Chieh Chen, George Papandreou, Florian Schroff, and Hartwig Adam. Rethinking atrous convolution for semantic image segmentation. *arXiv preprint arXiv:1706.05587*, 2017.
- [19] Junyoung Chung, Caglar Gulcehre, KyungHyun Cho, and Yoshua Bengio. Empirical evaluation of gated recurrent neural networks on sequence modeling. *arXiv preprint arXiv:1412.3555*, 2014.
- [20] Shuang Qiu, Yao Zhao, Jianbo Jiao, Yunchao Wei, and ShiKui Wei. Referring image segmentation by generative adversarial learning. *TMM*, 2019.
- [21] Hengcan Shi, Hongliang Li, Qingbo Wu, and King N. Ngan. Query reconstruction network for referring expression image segmentation. *TMM*, PP(99):1–1, 2020.
- [22] Jeffrey Pennington, Richard Socher, and Christopher D Manning. Glove: Global vectors for word representation. In *EMNLP*, pages 1532–1543, 2014.
- [23] Sahar Kazemzadeh, Vicente Ordonez, Mark Matten, and Tamara Berg. Referitgame: Referring to objects in photographs of natural scenes. In *EMNLP*, pages 787–798, 2014.
- [24] Junhua Mao, Jonathan Huang, Alexander Toshev, Oana Camburu, Alan L Yuille, and Kevin Murphy. Generation and comprehension of unambiguous object descriptions. In *CVPR*, pages 11–20, 2016.
- [25] Licheng Yu, Patrick Poirson, Shan Yang, Alexander C Berg, and Tamara L Berg. Modeling context in referring expressions. In *ECCV*, pages 69–85. Springer, 2016.
- [26] Mark Everingham, Luc Van Gool, Christopher KI Williams, John Winn, and Andrew Zisserman. The pascal visual object classes (voc) challenge. *IJCV*, 88(2):303–338, 2010.
- [27] Philipp Krähenbühl and Vladlen Koltun. Efficient inference in fully connected crfs with gaussian edge potentials. In *NeurIPS*, pages 109–117, 2011.